Beyond Shape Selective Catalysis with Zeolites: Hydrophobic Void Spaces in Zeolites Enable Catalysis in Liquid Water

Rajamani Gounder and Mark E. Davis
Chemical Engineering, California Institute of Technology, Pasadena, CA 91125

DOI 10.1002/aic.14016
Published online January 24, 2013 in Wiley Online Library (wileyonlinelibrary.com)

Zeolites confine active sites within void spaces of molecular dimension. The size and shape of these voids can be tuned by changing framework topology, which can influence catalytic reactivity and selectivity via coupled reaction-transport phenomena that exploit differences in transport properties among reactants and/or products that differ in size and shape. The polarity and solvating properties of intrazeolite void environments can be tuned by changing chemical composition and structure, ranging from hydrophobic defect-free pure-silica surfaces to silica surfaces containing hydrophilic defect sites and/or heteroatoms. Here, we discuss how the polarity of zeolite voids influences catalytic reactivity and selectivity via the partitioning of reactant, product, and solvent molecules between intrazeolitic locations and external fluid phases. These findings provide a conceptual basis for developing selective catalytic processes in aqueous media using hydrophobic zeolites that are able to adsorb organic reactants while excluding liquid water from internal void spaces. © 2013 American Institute of Chemical Engineers *AIChE J*, 59: 3349-3358, 2013
Keywords: hydrophobic, Lewis acid, tin-Beta, water-tolerant, zeolites

Introduction

We are delighted to contribute to this issue of the AIChE Journal dedicated to Professor Neal R. Amundson, who has made significant contributions to many different areas of chemical engineering over his career. Here, we discuss an emerging field in catalysis and reaction engineering that involves the coupling of transport with chemical reaction, an area of keen interest to Prof. Amundson. Specifically, we highlight how the hydrophobicity of zeolite voids can be tailored to control reactant and product partitioning into and out of microporous cavities that contain active sites, and how these effects can enable catalytic turnovers to proceed over active sites that are rendered inactive in aqueous media. Additionally, we draw analogies between reactions catalyzed within hydrophobic zeolite voids and those catalyzed within hydrophobic active site pockets of enzymes. The area of coupled transport and chemical reaction within hydrophobic pores is of increasing interest and relevance because the selective conversion of biomass into fuels and chemicals will likely involve catalytic reactions in aqueous media[1] and with Lewis acid centers[2] that tend to deactivate in water.[3,4] In the future, we envision possibilities to design catalytic processes that exploit both shape selectivity (based on size) and partitioning selectivity (based on polarity) using molecular sieves containing void spaces with selected topological features and solvation properties.

Zeolites and zeolite-like molecular sieves are crystalline solids with ordered and well-defined microporous void spaces that vary in size (~0.4–1.3 nm in pore diameter), topology (e.g., channels, pockets, cages), and interconnectivity. Zeolites, strictly aluminosilicates, contain tetrahedrally coordinated aluminum (Al^{3+}) and silicon atoms (Si^{4+}) that are connected by bridging oxygen atoms to create these three-dimensional frameworks, with a negative charge and a compensating extraframework cation per framework aluminum atom.[5,6] Proton-form zeolites (H-zeolites) are Brønsted acids and are prevalent in the petrochemical industry as solid acid catalysts for gas-phase hydrocarbon reactions.[7,8] Molecular sieves with different catalytic function can be obtained by the incorporation of other trivalent (e.g., B^{3+}, Ga^{3+}, and Fe^{3+}) or tetravalent (e.g., Ti^{4+}, Sn^{4+}, and Zr^{4+}) heteroatoms within pure-silica frameworks to form Brønsted acid sites or Lewis acid sites, respectively, and can also be derived from the presence of extraframework species (e.g., metals, metal oxides, and metal carbides).[9] The catalytic diversity of these materials is quite expansive even within a class of molecular sieves defined by a single catalytic function, because of the structural differences prevalent among crystalline frameworks (~200 in number)[10] and among the specific void spaces that contain active sites.[11,12]

One of the hallmarks of zeolite catalysis is shape selectivity based on the ability of microporous structures to discriminate molecules using size and shape criteria.[13,14] These shape-selective phenomena reflect the coupling of reaction and transport processes, because the confinement of active sites within microporous voids requires that reactants and products traverse void structures and that transition states form within constrained spaces in order for catalytic cycles to turn over. Weisz and co-workers first reported on these phenomena in the early 1960s (Scheme 1),[15,16] demonstrating that 1-butanol was dehydrated selectively over isobutanol

Correspondence concerning this article should be addressed to Mark E. Davis at mdavis@cheme.caltech.edu.

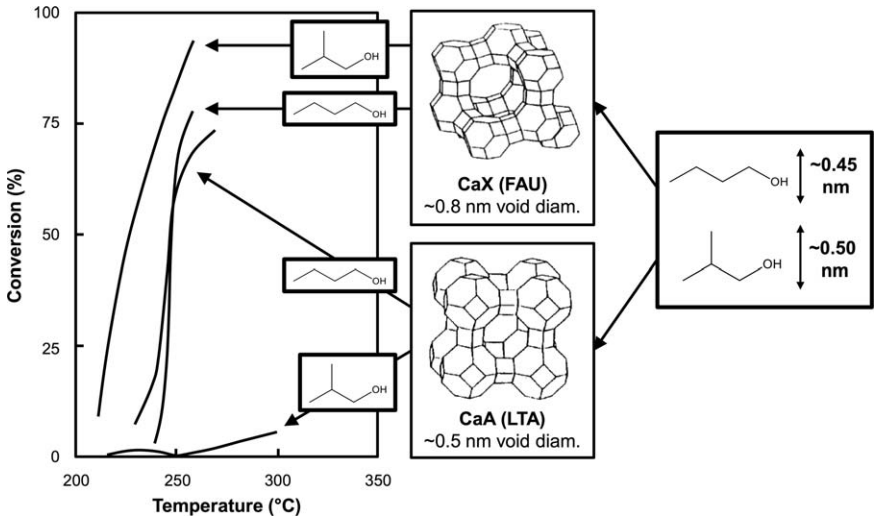

Scheme 1. The initial demonstration of shape-selective catalysis in the vapor-phase by Weisz et al.[15,16] showed that both 1-butanol and isobutanol dehydration was catalyzed by CaX, but that only 1-butanol dehydration was catalyzed by CaA; scheme adapted from Davis.[5]

(~0.45 and ~0.50 nm kinetic diameters, respectively[17,18]) in the vapor phase using acidic CaA (LTA; ~0.50 nm void diameter), but that such selectivity was not possible within the larger voids of CaX (FAU; ~0.80 nm void diameter) or amorphous SiO_2–Al_2O_3 (~10 nm void diameter). The ability to perform shape-selective catalysis using zeolites and zeolite-like molecular sieves creates numerous opportunities for combining catalysis and separation, and is exploited in many industrial reactions that occur predominantly at high-temperatures and in the vapor phase.[19–21]

The advent of synthetic protocols in the late 1970s to prepare molecular sieves with hydrophobic properties[22,23] has led to their investigation as catalysts for liquid-phase reactions. Shape selectivity can still be exploited for selective catalysis in condensed media, but the polarity of internal micropore surfaces can also be tuned to influence reactivity and selectivity via the partitioning of reactant, product, and solvent molecules between intrazeolite and extrazeolite phases. Thus, molecular sieves prepared with precise solvation properties have the potential to open new areas of combined reaction and separation in the liquid phase based on polarity, much in the same way that their pore architectures have been designed rationally to enable shape-selective catalysis in the vapor phase.[24] Here, we briefly discuss the synthesis and characterization of molecular sieve catalysts with hydrophobic properties and highlight two classes of reactions catalyzed by Lewis acid zeolites in aqueous media: alkene epoxidation and alkane oxidation with TS-1 (i.e., titanium silicalite-1, Ti-MFI) and aldose–ketose sugar isomerization with Ti-Beta and Sn-Beta. These examples highlight the roles of hydrophobic voids to influence the partitioning of reactants from condensed phases and to prevent framework Lewis acid centers from contact with bulk water. The ability to selectively perform reactions in liquid water[25,26] or two-phase water-organic mixtures[27–29] is of growing importance due to recent interest in utilizing biomass as a sustainable carbon source for fuels and chemicals.

Experimental Methods

Synthesis and characterization of zeolite samples

Procedures to synthesize Si-Beta-F,[30] Ti-Beta-F[31] (Si/Ti=196), Ti-Beta-OH[32] (Si/Ti=38), and Sn-Beta-F[33] (Si/Sn=87) were adapted from previously reported protocols. The TiO_2–SiO_2 sample used in this study is the TiO_2–SiO_2 co-precipitate (type III, no. 2) sample obtained from W.R. Grace (Si/Ti=56) that was used previously by Khouw et al.[34] to study hydrocarbon oxidation. After crystallization, zeolites were recovered by filtration, washed extensively with deionized and distilled water, and dried overnight at 373 K. The dried solids were calcined in flowing air (1.67 $cm^3\ s^{-1}$, Air Liquide, breathing grade) at 853 K (0.0167 K s^{-1}) for 10 h to remove the organic content within the crystalline material. The elemental compositions of all samples were determined using a JEOL 8200 electron microprobe operated at 15 kV and 25 nA in a focused beam mode with a 40 μm spot size. Scanning electron microscopy (SEM) images of zeolite samples were recorded on a LEO 1550 VP field emission SEM at an electron high tension of 10 kV.

Vapor-phase adsorption isotherms on zeolite samples

Vapor-phase adsorption isotherms for N_2 (77 K), H_2O (293 K), CH_3OH (293 K), and C_2H_5OH (293 K) were obtained using a Quantachrome Autosorb iQ automated gas sorption analyzer. Zeolite samples (typically 0.02–0.05 g) were first pelleted and sieved to retain 150–600 μm particles. Samples were then degassed at 353 K (0.167 K s^{-1}) for 1 h, 393 K (0.167 K s^{-1}) for 3 h, and 623 K (0.167 K s^{-1}) for 8 h prior to measurement of adsorption isotherms.

The micropore volume accessible to N_2, CH_3OH, and C_2H_5OH adsorbates was determined by analyzing the semi-log derivative plots of adsorption isotherms ($\partial(V_{ads}/g)/\partial(\log(P/P_0))$ vs. $\log(P/P_0)$). The relative pressure at which the micropore filling transition occurs in microporous solids is given by the first maximum of $\partial(V_{ads}/g)/\partial(\log(P/P_0))$; in turn, the local minimum that follows immediately corresponds to the end of micropore filling.[35,36] The total H_2O uptakes reported in Table 1 correspond to the volume of H_2O adsorbed at $P/P_0=0.2$ for comparison purposes, because micropore filling transitions were not detected for H_2O isotherms on hydrophobic materials. All values are reported as a micropore volume ($cm^3\ g^{-1}$), determined from the number of moles contained within the volume of adsorbed gas ($cm^3\ g^{-1}$ at STP) and the liquid molar density ($cm^3\ mol^{-1}$) of each adsorbate.

Table 1. Total Micropore Uptakes of N_2 (77 K), CH_3OH (293 K), and C_2H_5OH (293 K), and Total H_2O Uptakes at $P/P_0=0.2$ (293 K) on the Zeolite Samples in this Study

Catalyst	V_{ads} (N_2) ($cm^3\ g^{-1}$)[a]	V_{ads} (CH_3OH) ($cm^3\ g^{-1}$)[a]	V_{ads} (C_2H_5OH) ($cm^3\ g^{-1}$)[a]	V_{ads} (H_2O) ($cm^3\ g^{-1}$)[b]	V_{ads} (H_2O), normalized ($cm^3\ g^{-1}$)[c]
Si-Beta-F	0.19	0.19	0.22	0.0022	–
Ti-Beta-F	0.21	0.20	0.20	0.0024	0.0024
Sn-Beta-F	0.21	0.18	0.17	0.0093	0.0042
Ti-Beta-OH	0.22	0.18	0.19	0.076	0.015

[a]Uptake at end of micropore filling transition, determined from the minimum of $\partial(V_{ads}/g)/\partial(\log(P/P_0))$.
[b]Uptake at $P/P_0=0.2$.
[c]Uptake of H_2O normalized to an equivalent Si/M ratio (196), for comparison purposes.

Reaction and adsorption studies of glucose–water mixtures with Lewis acid zeolites

Glucose isomerization reactions on Sn-Beta and Ti-Beta catalysts were performed using experimental and analytical protocols reported elsewhere.[26,37] The reaction conditions used in this study were chosen to maintain differential conversion (<5%), in order to calculate initial turnover rates; typically, glucose/water solutions (1–10% (w/w)) were reacted over a catalyst (1:50 metal:glucose) at 373 K for less than 15 min. Turnover rates (per total metal atom) were calculated from the total moles of glucose converted.

Aqueous-phase glucose adsorption experiments were conducted in 10 mL thick-walled glass reactors (VWR) sealed with crimp tops that contained calcined zeolite samples and aqueous D-glucose (Sigma-Aldrich, ≥99%) solutions (1% or 0.25% (w/w); 50 $cm^3\ g_{cat}^{-1}$). The reactor contents were stirred at ambient temperature for 1 h, after which the solids were recovered by centrifugation and dried in ambient air overnight before characterization.

Simultaneous thermogravimetric analysis (TGA) and differential scanning calorimetry (DSC) was performed using a Netzsch STA 449 C instrument. Samples (~0.04 g) were placed in an alumina crucible and heated at 0.167 K s^{-1} in a flowing stream (0.667 $cm^3\ s^{-1}$) comprised of 50% air (Air Liquide, breathing grade) and 50% argon (Air Liquide, UHP).

^1H and ^{13}C solid-state magic angle spinning nuclear magnetic (MAS NMR) spectra were recorded on a Bruker Avance 500 MHz spectrometer equipped with a 11.7 T magnet and a Bruker 4mm MAS probe. Zeolite samples (0.06–0.08 g), after adsorption of glucose from aqueous solutions, were packed into 4 mm ZrO_2 rotors with Kel-F caps and spun at 14 kHz. ^1H and ^{13}C NMR spectra were recorded at operating frequencies of 500.2 and 125.8 MHz, respectively.

Results and Discussion

Synthesis and characterization of hydrophilic and hydrophobic molecular sieves

The direct synthesis of pure-silica frameworks using hydroxide anions as mineralizing agents leads to the formation of anionic framework vacancy defect sites (Scheme 2) that balance the cationic charges present in structure directing agents (R^+).[38–41] The removal of R^+ cations forms hydrophilic silanol nest defects (Scheme 2), which can be healed by chemical treatments that facilitate the reinsertion of mononuclear silicon complexes into framework vacancies.[39,42–44] In contrast to hydroxide-mediated crystallization, the use of fluoride anions as mineralizing agents (in the absence of alkali cations) forms zeolite crystals with low internal defect densities,[45] because F^- forms ion-pairs with cationic structure directors (R^+) and remain occluded within zeolite crystals (Scheme 2). The presence of F^- within microporous voids mitigates the formation of defect sites to maintain charge neutrality, in turn, leading to pure-silica molecular sieves that are very hydrophobic.

The amount of physisorbed water (298 K) on amorphous silica samples of varying silanol density reflects only a small fraction (0.13–0.25) of their total surface area determined by N_2 adsorption (78 K), but correlates well with the number of Si-OH groups estimated by infrared spectroscopy.[46] Mordenite (MOR) zeolites of varying Si/Al ratio (~80–200), prepared by extraction of framework Al atoms and healing of vacancy defects by acid treatments or by alternating acid and steam treatments, adsorb similar amounts of cyclohexane (298 K) but systematically less water (298 K) with decreasing Al content (Si/Al ~80–200).[43] These studies were among the first to demonstrate that defect-free regions of silica surfaces containing only nonpolar Si—O—Si bonds do not adsorb water vapor and are truly hydrophobic, but that defective Si-OH groups and OH groups at framework Al centers (Si-O(H)-Al) are hydrophilic and can adsorb molecular water. Thus, silica-based molecular sieves become less hydrophobic with increasing numbers of defect silanol groups or framework heteroatoms.

Debenedetti and co-workers have studied the phase behavior of water confined between hydrophobic and hydrophilic surfaces,[47–49] concluding that only vapor-phase water is present (at ambient pressures) between hydrophobic surfaces

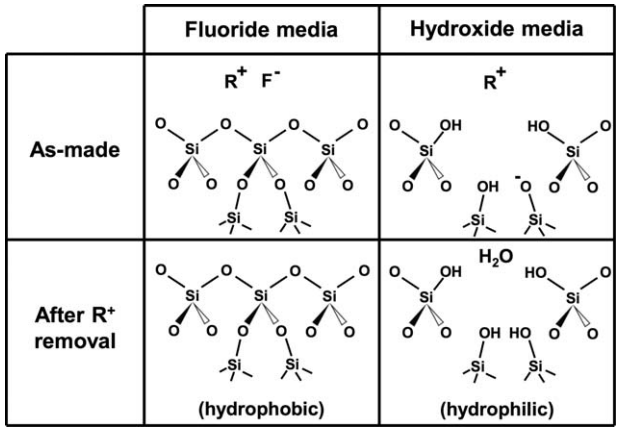

Scheme 2. Zeolite crystallization in fluoride media leads to silica surfaces that are essentially defect-free, nonpolar, and hydrophobic.

In contrast, crystallization in hydroxide media leads to framework vacancy defects that are more hydrophilic and adsorb water molecules and clusters.

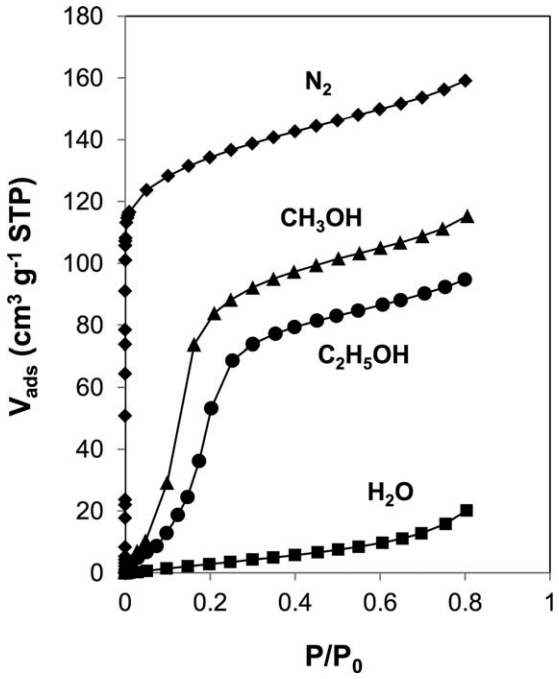

Figure 1. Adsorption isotherms for N_2 at 77 K: (◆), H_2O at 293 K (■), CH_3OH at 293 K (▲) and C_2H_5OH at 293 K (•) on Si-Beta-F.

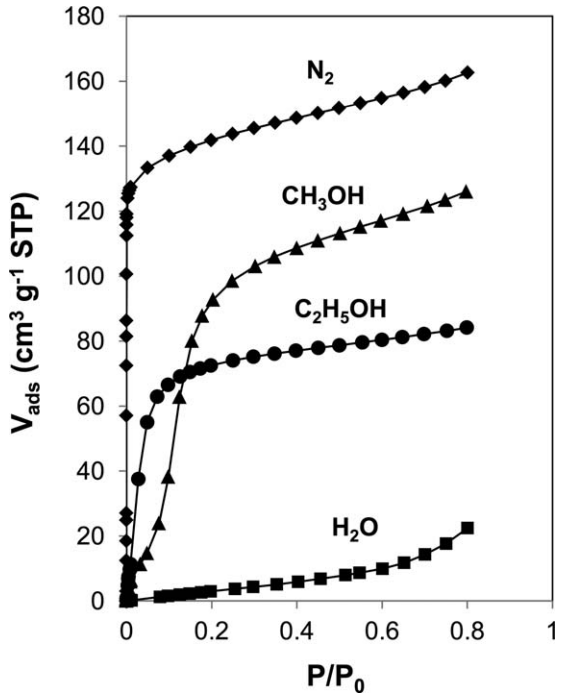

Figure 2. Adsorption isotherms for N_2 at 77 K: (◆), H_2O at 293 K (■), CH_3OH at 293 K (▲), and C_2H_5OH at 293 K (•) on Ti-Beta-F.

separated by distances of ~0.80 nm or less.[48] In agreement with the behavior predicted by Debenedetti[47–49] and coworkers,[50] experimental studies indicate that water intrusion (near ambient temperatures) into pure-silica MFI (~0.55 nm pore diameter) and BEA (~0.70 nm pore diameter) requires pressures of ca. 100 and 57 MPa, respectively.[51] Thus, while water molecules can adsorb at hydrophilic sites isolated within microporous voids of hydrophobic molecular sieves,[49,50,52] they are unable to form condensed phases or to fill internal micropore spaces smaller than ~0.80 nm in diameter under ambient conditions.

Single-component vapor-phase adsorption isotherms for nitrogen (77 K), water (293 K), methanol (293 K), and ethanol (293 K) on a pure-silica Beta zeolite synthesized in fluoride media (Si-Beta-F) are shown in Figure 1. The N_2 adsorption isotherm (Figure 1) corresponds to a Type I isotherm (micropore adsorption) with a total micropore volume of 0.19 $cm^3\ g^{-1}$ (Table 1). In contrast with the adsorption behavior of N_2, the H_2O isotherm on Si-Beta-F (Figure 1) corresponds to a Type III isotherm (weak adsorbate–adsorbent interactions) as expected for H_2O adsorption on a hydrophobic surface; H_2O uptakes were lower than the N_2 micropore volume by two orders-of-magnitude (0.0022 $cm^3\ g^{-1}$ at $P/P_0=0.2$; Table 1). The adsorption isotherms of CH_3OH and C_2H_5OH on Si-Beta-F (Figure 1) both followed Type V isotherms (weak adsorbate–adsorbent interactions with condensation driven by adsorbate–adsorbate interactions), with total micropore uptakes similar to the N_2 micropore volume (0.19 and 0.22 $cm^3\ g^{-1}$ respectively; Table 1). These data indicate that N_2, CH_3OH, and C_2H_5OH, *but not* H_2O, are able to fill the microporous voids of Si-Beta-F, as expected from the hydrophobic nature of pure-silica zeolites with low defect density.

As with defective silanol groups, framework heteroatoms such as Al (in MOR[43] and MFI[53]) and Ti (in MFI[54]) and extraframework alkali cations (in MFI[55]) also behave as hydrophilic centers that can adsorb water; specifically, each Ti center in Ti-Beta can adsorb two H_2O molecules.[56] We have synthesized Ti-Beta-F, Ti-Beta-OH, and Sn-Beta-F zeolites and report N_2, H_2O, CH_3OH, and C_2H_5OH isotherms on these samples in Figures 2–4, respectively. The amounts of N_2, CH_3OH, and C_2H_5OH adsorbed within the micropores of Ti-Beta-F, Ti-Beta-OH, and Sn-Beta-F were similar to

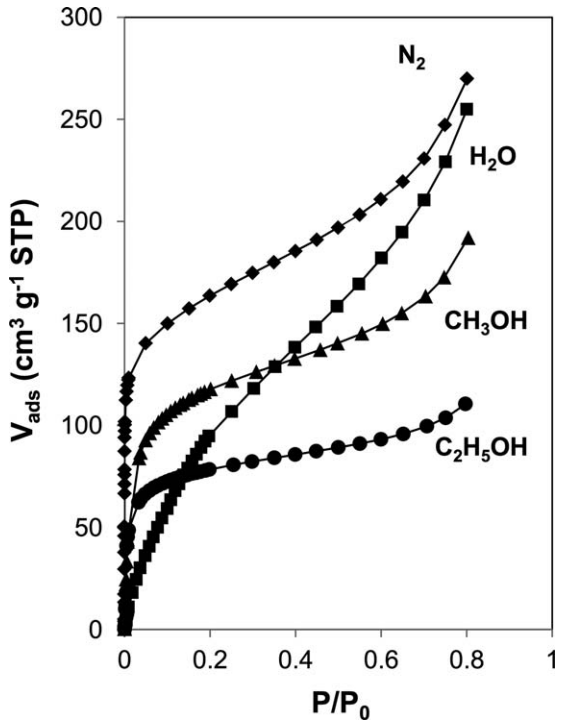

Figure 3. Adsorption isotherms for N_2 at 77 K: (◆), H_2O at 293 K (■), CH_3OH at 293 K (▲), and C_2H_5OH at 293 K (•) on Ti-Beta-OH.

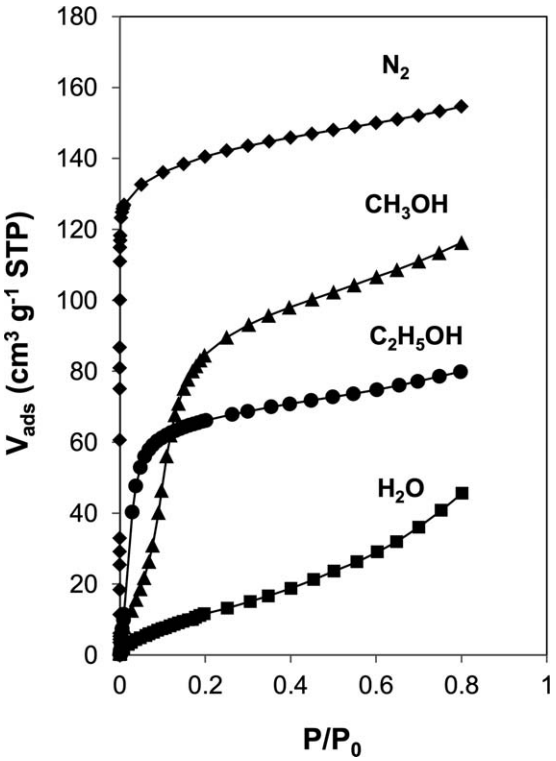

Figure 4. Adsorption isotherms for N_2 at 77 K: (◆), H_2O at 293 K (■), CH_3OH at 293 K (▲), and C_2H_5OH at 293 K (•) on Sn-Beta-F.

those on Si-Beta-F (Table 1). The H_2O uptake was negligible on Ti-Beta-F (0.0024 cm^3 g^{-1}; Table 1) and similar to that on hydrophobic Si-Beta-F, in sharp contrast with the higher (by a factor of ~32) H_2O uptake on defective Ti-Beta-OH (0.076 cm^3 g^{-1}; Table 1). Even after accounting for differences in Ti content, much larger amounts of H_2O were adsorbed on Ti-Beta-OH than on Ti-Beta-F (by a factor of >6; Table 1), consistent with the higher H_2O uptakes on Ti-Beta-OH than on Ti-Beta-F zeolites with similar Ti content reported previously.[32,56] The amount of H_2O adsorbed on Sn-Beta-F was higher than on Ti-Beta-F by a factor of 2 (at $P/P_0=0.2$, after accounting for differences in metal content; Table 1), which may reflect a higher density of internal bridging defects formed via preferential hydrolysis of Sn—O—Si bonds relative to Ti—O—Si bonds, or a larger number of external silanol groups on the smaller crystals of Sn-Beta-F (SEM images for all samples shown in Figure 5). These H_2O adsorption isotherms and the findings reported by others[32,43,53–56] suggest that, in addition to using fluoride and hydroxide anions to respectively prepare zeolites with very hydrophobic (Si-Beta-F, Ti-Beta-F) and hydrophilic (Ti-Beta-OH) properties, zeolite polarity can be tuned more precisely by changing heteroatom identity (Sn-Beta-F), amount, and coordination within zeolite frameworks.

The adsorption of methanol and ethanol, but not water, to the point of complete micropore filling in hydrophobic zeolites synthesized in fluoride media (Figures 1, 2, and 4) is analogous to the adsorption behavior reported on hydrophobic dealuminated Y zeolites[44] and on defect-free pure-silica MFI.[23,57] The single-component vapor-phase adsorption data reported in Figures 1–4 are also consistent with multiple-component liquid-phase adsorption experiments that have documented the organophilic character of hydrophobic zeolites (e.g., high-silica Al- and Ti-MFI zeolites), which cause the preferential adsorption of organic molecules (e.g., propanol,[40] butanol,[58] and *n*-octane[54]) from aqueous solutions. Therefore, the vapor-phase adsorption isotherms of solvent molecules (e.g., H_2O, CH_3OH) on zeolites and molecular sieves provide inferences, to an extent, about the ability of reactants (or products) to partition into (or out of) zeolite crystals from aqueous or organic solvents. These data suggest that hydrophobic zeolite channels that exclude bulk water under typical operating conditions (<50 MPa) should enable the selective adsorption, transport, and catalysis of organic molecules in liquid water, as we discuss next.

Alkene epoxidation and alkane oxidation catalysis on Ti-zeolites in the liquid phase

The applications of Ti-containing heterogeneous catalysts for liquid-phase oxidation reactions of alkanes and alkenes, in which Ti centers behave as Lewis acids that coordinate and activate peroxide oxidants, have been reviewed extensively.[59–61] Isolated Ti centers dispersed on amorphous silica (TiO_2–SiO_2) were heterogeneous catalysts used by Shell in the 1970s, and can catalyze oxidation reactions when organic hydroperoxides or anhydrous H_2O_2 are used as oxidants.[34,62] Amorphous TiO_2–SiO_2 deactivates rapidly when aqueous H_2O_2 is used as the oxidant,[34] however, because hydrophilic silanol groups adsorb large amounts of H_2O (~50 wt% water when exposed to humid air[34]) that coordinates strongly with Ti[59,60] to inhibit catalytic turnovers.[3,4]

The discovery of TS-1, the first material reported to activate H_2O_2 as an oxidant in aqueous media,[63,64] opened several new opportunities for oxidation catalysis in water with TS-1[60] and with other titanosilicates, including Ti-SSZ-33,[65] Ti-Beta[66], and Ti-MCM-41.[67] As with TiO_2–SiO_2 materials that contain active isolated Ti centers supported on amorphous silica, TS-1 contains isolated Ti centers located within the framework of crystalline silicalite (MFI). In contrast with the hydrophilic environment surrounding Ti centers in TiO_2–SiO_2, however, the microporous voids that confine Ti centers

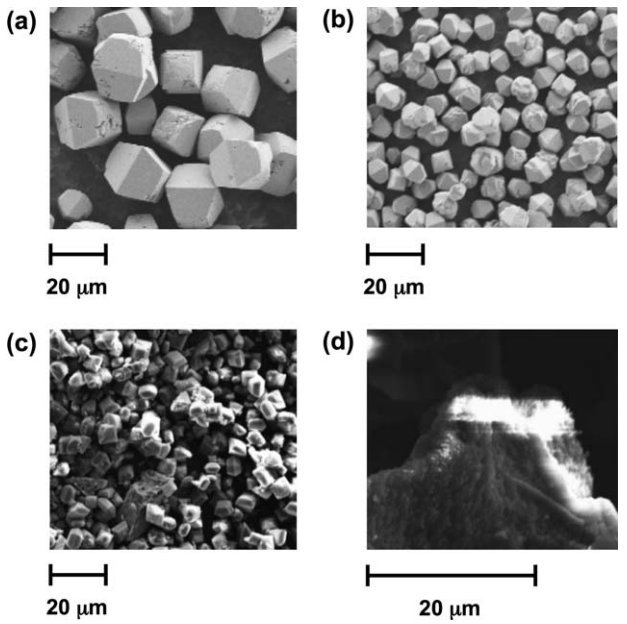

Figure 5. SEM images of (a) Si-Beta-F crystals, (b) Ti-Beta-F crystals, (c) Sn-Beta-F crystals, and (d) Ti-Beta-OH crystal agglomerates.

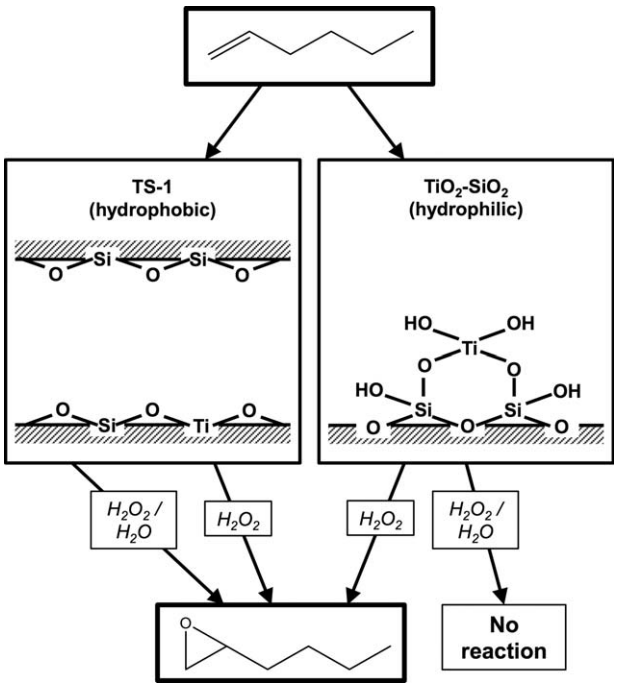

Scheme 3. 1-Hexene epoxidation to 1,2-epoxyhexane using aqueous H_2O_2 as the oxidant is catalyzed by isolated Ti centers located within hydrophobic TS-1 micropores, but not at more hydrophilic TiO_2–SiO_2 surfaces; in contrast, both TS-1 and TiO_2–SiO_2 catalyze epoxidation in anhydrous H_2O_2. Active site structure for TiO_2–SiO_2 adapted from Dusi et al.[59]

Epoxidation data reported by Khouw et al.[34]

in essentially defect-free TS-1 are hydrophobic (Scheme 3). TS-1 shows nearly identical conversion for both 1-hexene epoxidation and *n*-octane oxidation in aqueous and anhydrous H_2O_2, yet TiO_2–SiO_2 shows nearly an order-of-magnitude lower conversion in aqueous than anhydrous H_2O_2 (Scheme 3).[34] This behavior reflects the ability of hydrophobic TS-1 channels to prevent liquid water from contacting with and inhibiting catalytic turnovers at Lewis acidic Ti centers, as occurs at the Ti sites located on the amorphous and hydrophilic surfaces of TiO_2–SiO_2.[34]

Although TS-1 is able to catalyze alkene epoxidation reactions using aqueous H_2O_2, initial reaction rates are higher in methanol solvent[68,69] and vary in other polar (e.g., alkanols) and aprotic (e.g., acetonitrile, acetone) solvents,[70–73] which influence reactant partition coefficients and intrazeolite reactant concentrations. Langhendries et al.[70] reported that 1-hexene epoxidation rates on TS-1 (~0.55 nm void diameter) with H_2O_2 in different alkanol solvents (methanol, ethanol, and 1-propanol) increased systematically with 1-hexene partition coefficients. The differences in 1-hexene partition coefficients, and initial epoxidation rates in turn, among these alkanol solvents were less pronounced on Ti/Al-Beta (~0.70 nm void diameter) and Ti-MCM-41 (>1.6 nm void diameter) than on TS-1, because van der Waals interactions between confined alkene reactants and zeolite pore walls become less effective with increasing void size.[70] Ramachandran et al.[73] also ascribed differences in initial 1-hexene epoxidation rates on TS-1 with H_2O_2 in methanol, acetone, and acetonitrile solvents predominantly, but not exclusively, to differences in 1-hexene partition coefficients. Clerici[71] studied *n*-hexane oxidation on TS-1 with H_2O_2 in different solvents (water, methanol, acetonitrile, *t*-butanol, and *t*-butanol/water) and reported that initial *n*-hexane oxidation rates and *n*-hexane partition coefficients showed *opposite* dependences on solvent identity.

The contrasting effects of solvent identity on the rates of alkane oxidation[71] and alkene epoxidation,[70,72,73] relative to their respective reactant partition coefficients, highlight the complex and oftentimes convoluted effects of solvent molecules on catalysis. Solvent molecules interact with reactants and products to influence the thermodynamics of their partitioning between liquid and solid phases and the dynamics of their transport within zeolite channels. Solvent molecules also coordinate with active sites or with adsorbed intermediates bound at such sites to influence the dynamics of catalytic reactions. Although the mechanistic origins of the solvent effects in epoxidation catalysis continue to be investigated, the demonstration that TS-1 can catalyze epoxidation in aqueous H_2O_2 provides evidence that Lewis acid centers are protected from inhibition by bulk water when they are confined within hydrophobic voids. This appears to be a general feature of catalysis by hydrophobic Lewis acid zeolites in liquid water, as we discuss next in the context of sugar isomerization.

Sugar isomerization on hydrophobic Ti- and Sn-zeolites in water

The isomerization of glucose to fructose is a reaction that enables the production of high fructose corn syrup, currently the largest immbolized biocatalytic process worldwide,[74] and is a critical step in the conversion of lignocellulosic biomass to valuable chemical intermediates. Homogeneous base catalysts can be used to catalyze aldose–ketose isomerization reactions on an industrial scale, yet they also mediate undesired sugar degradation side reactions and require subsequent product separation and purification steps.[74] Although certain enzymes (e.g., phosphoglucose isomerase) contain basic amino acid residues that catalyze glucose isomerization via enediol intermediates,[75,76] industrially-used metalloenzymes (e.g., D-xylose isomerase XI)[74] contain two Lewis acidic divalent metal ions (e.g., Mg^{2+}, Mn^{2+}) that mediate the ring opening of glucose and the subsequent intramolecular hydride shift from C-2 to C-1 positions on the glucose backbone in isomerization steps.[77,78] Lewis-acid mediated pathways obviate the selectivity problems associated with the formation of enolate species in homogeneous media, but isomerase metalloenzymes operate optimally within narrow pH (~7–9) and temperature (~333–353 K) ranges and with feeds containing low impurity concentrations.[74] Therefore, a water-tolerant heterogeneous Lewis acid catalyst would avoid base-catalyzed degradation side-reactions and also enable glucose isomerization at temperatures higher than 353 K, which are more favorable thermodynamically for fructose production but are incompatible with enzyme catalysts.

Pure-silica zeolite frameworks containing Ti and Sn centers behave as solid Lewis acids, including the hydrophobic TS-1 materials used for oxidation catalysis in aqueous media.[34,60,63,64] Lewis acid zeolites with the MFI topology (e.g., TS-1), however, do not catalyze glucose isomerization[26] because their active centers are located within pores (~0.55 nm diameter) too small to accommodate glucose reactants (~0.85 nm diameter[79]). Ti-Beta and Sn-Beta

Table 2. Turnover Rates for Glucose Isomerization to Fructose (373 K) in H_2O Solvent, and the Ratio of H_2O-to-N_2 Uptakes on Lewis Acid Zeolites and TiO_2–SiO_2

Catalyst	Isomerization turnover rate (mol [(mol metal)-s]$^{-1}$)	V_{ads} (H_2O)/ V_{ads} (N_2)
Sn-Beta-F	0.0278±0.0050	0.044
Ti-Beta-F	0.0011±0.0001	0.011
Ti-Beta-OH	n.d.[a]	0.35
TiO_2–SiO_2	n.d.[a]	0.30

[a]n.d. not detected.

zeolites contain pores (~0.70 nm diameter) of similar size to glucose and also behave as Lewis acids that catalyze the Baeyer–Villiger oxidation and Meerwein–Ponndorf–Verley (MPV) reduction of carbonyl compounds in organic media.[80–82] Indeed, the isomerization of glucose to fructose occurs on hydrophobic Ti-Beta-F and Sn-Beta-F zeolites in water,[26] via a Lewis-acid catalyzed intramolecular hydride shift mechanism analogous to that which prevails on metalloenzymes.[83,84] The polarity of channels in zeolite Beta should, by extension of its effects on hydrocarbon oxidation, influence glucose isomerization catalysis via the partitioning of glucose reactant and water solvent molecules.

Sn-Beta-F contains hydrophobic voids with framework Sn centers that isomerize glucose (Table 2),[26,37] indicating that sugar molecules are able to adsorb and react within hydrophobic channels even though bulk water is excluded from them (Figure 4). We probed these adsorption properties by contacting aqueous solutions of glucose (1% and 0.25% (w/w)) with Sn-Beta-F at ambient temperature, after which the solids were recovered and analyzed by simultaneous TGA/DSC and by ^{13}C and ^{1}H MAS NMR spectroscopies. Thermogravimetric analysis of the Sn-Beta-F sample contacted with a 1% (w/w) aqueous glucose solution showed a mass loss of ~3.4 wt% that was entirely exothermic (Figure 6a), reflecting solely the combustion of glucose (exothermic) with undetectable desorption of water (endothermic). Additionally, a ~3.5-fold difference in adsorbed glucose was detected in ^{13}C MAS NMR spectra (Figure 7a) of Sn-Beta-F samples exposed to 1% and 0.25% (w/w) aqueous glucose solutions, while the corresponding ^{1}H NMR spectra (Figure 7b) showed similar amounts of adsorbed H_2O located predominantly at external crystal silanol groups. The vapor-phase H_2O adsorption isotherm on Sn-Beta-F (Figure 4) and the TGA/DSC and NMR spectroscopic analyses of glucose adsorbed onto Sn-Beta-F from the aqueous-phase (Figures 6 and 7) provide evidence that glucose can adsorb and diffuse within hydrophobic zeolite channels in the absence of a condensed intrazeolitic water phase (Scheme 4). These adsorption and diffusion phenomena are mediated by the solvation of hexose sugars by van der Waals interactions with zeolitic framework oxygen atoms ($\Delta H_{ads} \sim -130$ kJ mol^{-1}

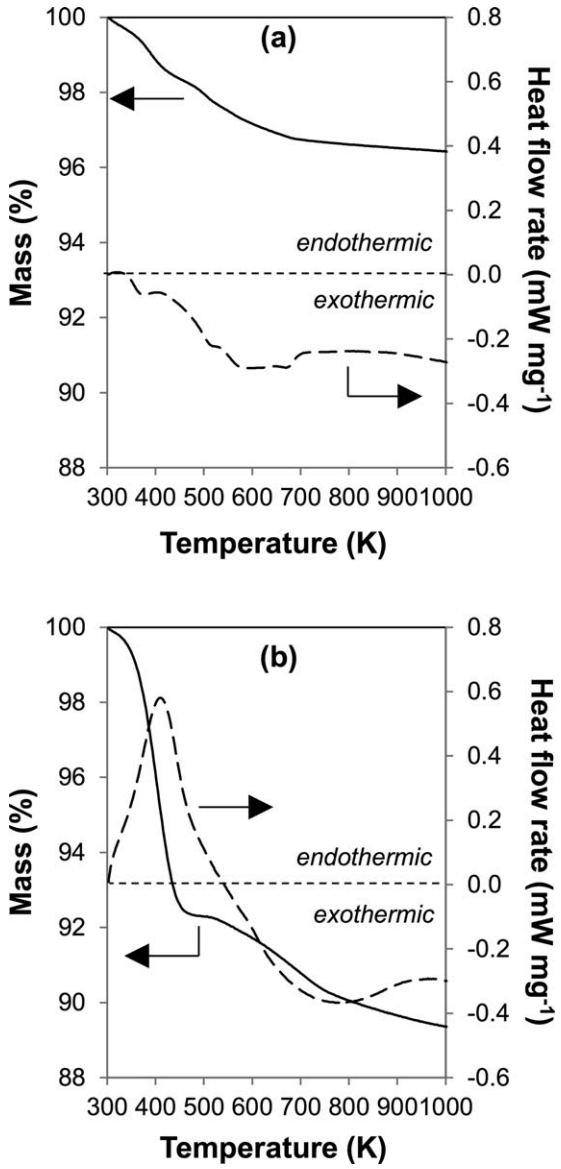

Figure 6. Mass (solid lines) and heat (dashed lines) flow changes during simultaneous TGA/DSC of calcined (a) Sn-Beta-F and (b) Ti-Beta-OH samples after contacting with a 1% (w/w) aqueous glucose solution.

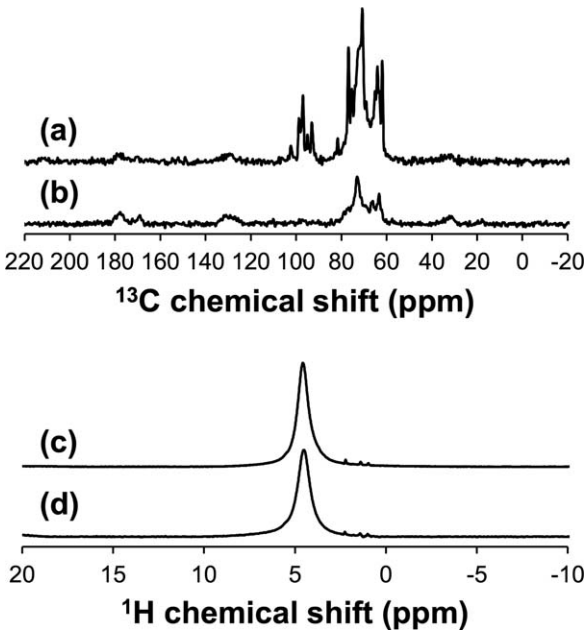

Figure 7. ^{13}C MAS NMR spectra of Sn-Beta-F after contacting with (a) 1% (w/w) and (b) 0.25% (w/w) aqueous glucose solutions; corresponding ^{1}H MAS NMR spectra are shown in (c) and (d), respectively.

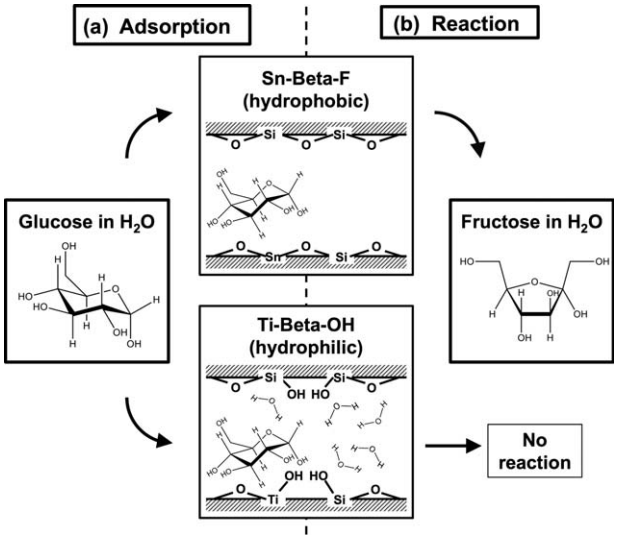

Scheme 4. (a) The adsorption of glucose from aqueous solutions into hydrophobic zeolite channels (e.g., Sn-Beta-F) occurs without the adsorption of water, but into hydrophilic zeolite channels (e.g., Ti-Beta-OH) occurs with concomitant water adsorption (Figures 6 and 7); (b) glucose isomerization to fructose in aqueous media occurs at Lewis acid centers confined within hydrophobic voids, but not at those confined within hydrophilic voids (Table 2).

estimated by theory for fructose in MFI[85]), which replace the hydrogen bonding interactions between sugar and water molecules in hydration shells present in bulk solution.

The defective channel environments of Ti-Beta-OH are much more hydrophilic than the essentially defect-free channels of Sn-Beta-F and Ti-Beta-F, and thus adsorb much larger quantities of water (Figure 3, Table 1). Thermogravimetric analysis of the Ti-Beta-OH sample after the adsorption glucose from a 1% (w/w) aqueous glucose solution showed an endothermic mass loss of ~7.9 wt% below 573 K and an exothermic mass loss of ~2.0 wt% above 573 K (Figure 6b). This endothermic mass loss below 573 K, which is absent on Sn-Beta-F (Figure 6a), reflects the desorption of physisorbed water. The amount of adsorbed water on Ti-Beta-OH (H_2O:glucose ~40) far exceed those required solely for the hydration of glucose in bulk solution (H_2O:glucose ~10)[86], indicating that a large fraction of the adsorbed H_2O resides within microporous spaces that did not contain glucose.

Glucose isomerized to fructose on both Sn-Beta-F and Ti-Beta-F, but glucose conversion remained below detection limits (<0.1%) on Ti-Beta-OH and TiO_2–SiO_2 (Table 2) under equivalent reaction conditions (1:50 total metal:glucose, 353 K, 15 min) and even at much longer reaction times (>1 h). These data indicate that framework Lewis acidic Ti and Sn centers are able to catalyze glucose isomerization in aqueous media when they are confined in hydrophobic channels of Beta zeolite, but not when located within hydrophilic void spaces or at hydrophilic surfaces of TiO_2–SiO_2. The hydrophobic channels of Ti-Beta-F and Sn-Beta-F screen bulk water from filling microporous voids (Scheme 4), in turn, preventing inhibition of Lewis acidic framework Ti and Sn centers during sugar isomerization. These findings are analogous to the ability of Lewis acidic framework Ti centers to catalyze oxidations in aqueous H_2O_2 when located in hydrophobic channels of TS-1, but not at hydrophilic surfaces of TiO_2–SiO_2.[34]

The role of hydrophobic zeolite channels to exclude liquid water from contacting active sites is also reminiscent of the role of hydrophobic amino acid residues (e.g., aromatic substituents on tryptophan and phenylalanine residues in D-xylose isomerase) to exclude water from metalloenzyme active site pockets during glucose isomerization.[77] Mechanistic studies with D-glucose isomerase have shown that the equilibration of unlabeled glucose–fructose mixtures in D_2O occurs without deuterium incorporation into the products.[87] Furthermore, the isomerization of glucose with deuterium labeled on C-1 and C-2 carbon atoms forms fructose with deuterium atoms located at C-1-S and C-1-R positions, respectively.[87] These two observations provide evidence that water solvent molecules do not scramble the hydride shared between glucose C-1 and C-2 atoms during isomerization and do not catalyze the mutarotation of the fructose products formed.[77] We suggest that the hydrophobic pockets of biological metalloenzymes, which exclude water molecules during glucose ring-opening and isomerization, also play a critical role to prevent inhibition of the divalent Lewis acidic metal cations that mediate these steps, similar to the effects of hydrophobic void environments that confine and protect Lewis acid sites in synthetic zeolites.

Summary

The synthesis of pure-silica zeolite structures using fluoride anions in synthesis mixtures has opened the pathway to the creation of numerous molecular sieves with low defect densities and hydrophobic properties. In amorphous and crystalline forms of pure silica, only defect-free surfaces comprised of nonpolar Si—O—Si bonds are truly hydrophobic, but such surfaces are inert catalytically. Heteroatoms incorporated into zeolite frameworks behave as catalytic active sites, but are hydrophilic and can bind molecular water. These active sites can be located within surrounding void environments that are essentially defect-free and hydrophobic, which prevents the condensation of bulk water within intracrystalline void spaces, or environments that are highly-defective and hydrophilic, which enables the adsorption of much larger quantities of water. Thus, tuning parameters that control the genesis of hydrophilic sites (e.g., F^- to OH^- ratio, heteroatom content) during the synthesis of silica-based molecular sieves, in turn, enables tuning the polarity of zeolite voids.

The hydrophobic properties of molecular sieves can be probed by vapor-phase water adsorption isotherms and by glucose adsorption from the aqueous phase. These methods demonstrate that zeolites with very low defect density synthesized in fluoride media adsorb significantly fewer water molecules (by an order-of-magnitude) than those with higher defect density synthesized in hydroxide media. Hydrophobic channels screen out bulk water but still adsorb organic reactants (e.g., glucose) that are normally solvated by waters of hydration in solution, because framework oxygen atoms solvate confined molecules by van der Waals interactions. Moreover, these hydrophobic void spaces confine and protect Lewis acid sites, which deactivate rapidly in the presence of liquid water, and enable them to catalyze hydrocarbon oxidation and sugar isomerization reactions in aqueous media.

These findings suggest that hydrophobic zeolites provide a useful synthetic platform to prepare site-isolated, water-tolerant solid Lewis acid catalysts[2,4] with the potential to catalyze reactions in aqueous media, for which hydrophilic solids or homogeneous complexes containing Lewis acid centers are not functional.

Acknowledgments

This work was financially supported as part of the Catalysis Center for Energy Innovation, an Energy Frontier Research Center funded by the US Department of Energy, Office of Science, Office of Basic Energy Sciences under Award Number DE-SC0001004. We thank Dr. Son-Jong Hwang for the ^{13}C and ^{1}H NMR spectra, Yashodhan Bhawe for helpful technical discussion, and Ricardo Bermejo-Deval and Carly Bond for experimental assistance.

Literature Cited

1. Huber GW, Iborra S, Corma A. Synthesis of transportation fuels from biomass: Chemistry, catalysts, and engineering. *Chem Rev*. 2006;106(9):4044–4098.
2. Román-Leshkov Y, Davis ME. Activation of carbonyl-containing molecules with solid Lewis acids in aqueous media. *ACS Catal*. 2011;1(11):1566–1580.
3. Corma A, Garcia H. Lewis acids: from conventional homogeneous to green homogeneous and heterogeneous catalysis. *Chem Rev*. 2003;103(11):4307–4365.
4. Okuhara T. Water-tolerant solid acid catalysts. *Chem Rev*. 2002;102(10):3641–3665.
5. Davis ME. Zeolites and molecular sieves – not just ordinary catalysts. *Ind Eng Chem Res*. 1991;30(8):1675–1683.
6. Davis ME. New vistas in zeolite and molecular sieve catalysis. *Acc Chem Res*. 1993;26(3):111–115.
7. Corma A. Inorganic solid acids and their use in acid-catalyzed hydrocarbon reactions. *Chem Rev*. 1995;95(3):559–614.
8. Venuto PB. Organic catalysis over zeolites: a perspective on reaction paths within micropores. *Microporous Mater*. 1994;2(5):297–411.
9. Lobo R. Chemical diversity of zeolite catalytic sites. *AIChE J*. 2008;54(6):1402–1409.
10. Baerlocher C, McCusker LB. Database of zeolite structures. Available at: http://www.iza-structure.org/databases/. Accessed December 10, 2012.
11. Bhan A, Iglesia E. A link between reactivity and local structure in acid catalysis on zeolites. *Acc Chem Res*. 2008;41(4):559–567.
12. Gounder R, Iglesia E. Catalytic consequences of spatial constraints and acid site location for monomolecular alkane activation on zeolites. *J Am Chem Soc*. 2009;131(5):1958–1971.
13. Csicsery SM. Shape-selective catalysis in zeolites. *Zeolites*. 1984;4(3):202–213.
14. Degnan TF. The implications of the fundamentals of shape selectivity for the development of catalysts for the petroleum and petrochemical industries. *J Catal*. 2003;216(1–2):32–46.
15. Weisz PB, Frilette VJ. Intracrystalline and molecular-shape-selective catalysis by zeolite salts. *J Phys Chem*. 1960;64(3):382–382.
16. Weisz PB, Frilette VJ, Maatman RW, Mower EB. Catalysis by crystalline aluminosilicates. 2. Molecular-shape selective reactions. *J Catal*. 1962;1(4):307–312.
17. Millot B, Methivier A, Jobic H, Moueddeb H, Dalmon JA. Permeation of linear and branched alkanes in ZSM-5 supported membranes. *Microporous Mesoporous Mater*. 2000;38(1):85–95.
18. van Leeuwen ME. Derivation of Stockmayer potential parameters for polar fluids. *Fluid Phase Equilib*. 1994;99:1–18.
19. Chen NY, Garwood WE. Industrial application of shape-selective catalysis. *Catal Rev-Sci Eng*. 1986;28(2–3):185–264.
20. Vermeiren W, Gilson JP. Impact of zeolites on the petroleum and petrochemical industry. *Top Catal* 2009;52(9):1131–1161.
21. van Bekkum H, Kouwenhoven HW. *Zeolite Manual for the Organic Chemist*. Delft: Mijnbestseller.nl; 2012.
22. Flanigen EM, Patton RL. Silica polymorph and process for preparing the same. U.S. Patent 4,073,865, 1978.
23. Flanigen EM, Bennett JM, Grose RW, Cohen JP, Patton RL, Kirchner RM, Smith JV. Silicalite, a new hydrophobic crystalline silica molecular-sieve. *Nature*. 1978;271(5645): 512–516.
24. Davis ME. Reaction chemistry and reaction engineering principles in catalyst design. *Chem Eng Sci*. 1994;49(24A):3971–3980.
25. da Silva CXA, Goncalves VLC, Mota CJA. Water-tolerant zeolite catalyst for the acetalisation of glycerol. *Green Chem*. 2009;11(1):38–41.
26. Moliner M, Román-Leshkov Y, Davis ME. Tin-containing zeolites are highly active catalysts for the isomerization of glucose in water. *Proc Natl Acad Sci USA*. 2010;107(14):6164–6168.
27. Zapata PA, Faria J, Ruiz MP, Jentoft RE, Resasco DE. Hydrophobic zeolites for biofuel upgrading reactions at the liquid-liquid interface in water/oil emulsions. *J Am Chem Soc*. 2012;134(20):8570–8578.
28. Nikolla E, Román-Leshkov Y, Moliner M, Davis ME. "One-pot" synthesis of 5-(hydroxymethyl)furfural from carbohydrates using tin-Beta zeolite. *ACS Catal*. 2011;1(4):408–410.
29. Camblor MA, Corma A, Iborra S, Miquel S, Primo J, Valencia S. Beta zeolite as a catalyst for the preparation of alkyl glucoside surfactants: the role of crystal size and hydrophobicity. *J Catal*. 1997;172(1):76–84.
30. Camblor MA, Corma A, Valencia S. Spontaneous nucleation and growth of pure silica zeolite-Beta free of connectivity defects. *Chem Commun*. 1996(20):2365–2366.
31. Camblor MA, Costantini M, Corma A, et al. Synthesis and catalytic activity of aluminium-free zeolite Ti-Beta oxidation catalysts. *Chem Commun*. 1996(11):1339–1340.
32. Camblor MA, Corma A, Esteve P, Martinez A, Valencia S. Epoxidation of unsaturated fatty esters over large-pore Ti-containing molecular sieves as catalysts: Important role of the hydrophobic–hydrophilic properties of the molecular sieve. *Chem Commun*. 1997(8):795–796.
33. Valencia S, Corma A. Stannosilicate molecular sieves. U.S. Patent 5,968,473, 1999.
34. Khouw CB, Dartt CB, Labinger JA, Davis ME. Studies on the catalytic oxidation of alkanes and alkenes by titanium silicates. *J Catal*. 1994;149(1):195–205.
35. Borghard WS, Reischman PT, Sheppard EW. Argon sorption in ZSM-5. *J Catal*. 1993;139(1):19–23.
36. Borghard WS, Sheppard EW, Schoennagel HJ. An automated, high-precision unit for low-pressure physisorption. *Rev Sci Instr*. 1991;62(11):2801–2809.
37. Bermejo-Deval R, Gounder R, Davis ME. Framework and extraframework tin sites in zeolite beta react glucose differently. *ACS Catal*. 2012;2:2705–2713.
38. Zecchina A, Bordiga S, Spoto G, Marchese L, Petrini G, Leofanti G, Padovan M. Silicalite characterization. 2. IR spectroscopy of the interaction of CO with internal and external hydroxyl groups. *J Phys Chem*. 1992;96(12):4991–4997.
39. Fickel DW, Shough AM, Doren DJ, Lobo RF. High-temperature dehydrogenation of defective silicalites. *Microporous Mesoporous Mater*. 2010;129(1–2):156–163.
40. Guth JL, Kessler H, Higel JM, Lamblin JM, Patarin J, Seive A, Chezeau JM, Wey R. Zeolite synthesis in the presence of fluoride ions – a comparison with conventional synthesis methods. *ACS Symp Ser*. 1989;398:176–195.
41. Shantz DF, Gunne J, Koller H, Lobo RF. Multiple-quantum H-1 MAS NMR studies of defect sites in as-made all-silica ZSM-12 zeolite. *J Am Chem Soc*. 2000;122(28):6659–6663.
42. Jones CW, Hwang SJ, Okubo T, Davis ME. Synthesis of hydrophobic molecular sieves by hydrothermal treatment with acetic acid. *Chem Mater*. 2001;13(3):1041–1050.
43. Chen NY. Hydrophobic properties of zeolites. *J Phys. Chem*. 1976;80(1):60–64.
44. Halasz I, Kim S, Marcus B. Uncommon adsorption isotherm of methanol on a hydrophobic Y-zeolite. *J Phys Chem B*. 2001;105(44):10788–10796.
45. Koller H, Lobo RF, Burkett SL, Davis ME. SiO-center-dot-center-dot-center-dot-HOSi hydrogen-bonds in as-synthesized high-silica zeolites. *J Phys Chem*. 1995;99(33):12588–12596.
46. Young GJ. Interaction of water vapor with silica surfaces. *J Colloid Sci*. 1958;13:67–85.
47. Giovambattista N, Rossky PJ, Debenedetti PG. Effect of temperature on the structure and phase behavior of water confined by hydrophobic, hydrophilic, and heterogeneous surfaces. *J Phys Chem B*. 2009;113(42):13723–13734.

48. Giovambattista N, Rossky PJ, Debenedetti PG. Effect of pressure on the phase behavior and structure of water confined between nanoscale hydrophobic and hydrophilic plates. *Phys Rev E*. 2006;73(4):041604.
49. Giovambattista N, Debenedetti PG, Rossky PJ. Hydration behavior under confinement by nanoscale surfaces with patterned hydrophobicity and hydrophilicity. *J Phys Chem C*. 2007;111(3):1323–1332.
50. Trzpit M, Soulard M, Patarin J, Desbiens N, Cailliez F, Boutin A, Demachy I, Fuchs AH. The effect of local defects on water adsorption in silicalite-1 zeolite: A joint experimental and molecular simulation study. *Langmuir*. 2007;23(20):10131–10139.
51. Eroshenko V, Regis RC, Soulard M, Patarin J. The heterogeneous systems 'water-hydrophobic zeolites': new molecular springs. *Comp Rend Phys*. 2002;3(1):111–119.
52. Cailliez F, Stirnemann G, Boutin A, Demachy I, Fuchs AH. Does water condense in hydrophobic cavities? A molecular simulation study of hydration in heterogeneous nanopores. *J Phys Chem C*. 2008;112(28):10435–10445.
53. Olson DH, Haag WO, Lago RM. Chemical and physical-properties of the ZSM-5 substitutional series. *J Catal*. 1980;61(2):390–396.
54. Weitkamp J, Ernst S, Roland E, Thiele GF. The modified hydrophobicity index as a novel method for characterizing the surface properties of titanium silicalites. In: Chon H, Ihm S-K, Uh YS, eds. *Progress in Zeolite and Microporous Materials, pts a-c*. Vol. 105. Amsterdam: Elsevier Science Publ B V, 1997:763–770.
55. Jentys A, Warecka G, Derewinski M, Lercher JA. Adsorption of water on ZSM5 zeolites. *J Phys Chem*. 1989;93(12):4837–4843.
56. Blasco T, Camblor MA, Corma A, Esteve P, Guil JM, Martínez M, Perdigón-Melón JA, Valencia S. Direct synthesis and characterization of hydrophobic aluminum-free Ti-Beta zeolite. *J Phys Chem B*. 1998;102(1):75–88.
57. Zhang K, Lively RP, Noel JD, Dose ME, McCool BA, Chance RR, Koros WJ. Adsorption of water and ethanol in MFI-type zeolites. *Langmuir*. 2012;28(23):8664–8673.
58. Dessau RM. Selective sorption properties of zeolites. *ACS Symp Ser*. 1980;135:123–135.
59. Dusi M, Mallat T, Baiker A. Epoxidation of functionalized olefins over solid catalysts. *Catal Rev-Sci Eng*. 2000;42(1–2):213–278.
60. Notari B. Microporous crystalline titanium silicates. *Adv Catal*. 41;1996:253–334.
61. Saxton RJ. Crystalline microporous titanium silicates. *Top. Catal*. 1999;9(1–2):43–57.
62. Sheldon RA, Vandoorn JA, Schram CWA, Dejong AJ. Metal-catalyzed epoxidation of olefins with organic hydroperoxides. 2. Effect of solvent and hydroperoxide structure. *J Catal*. 1973;31(3):438–443.
63. Taramasso M, Perego G, Notari B. Preparation of porous crystalline synthetic material comprised of silicon and titanium oxides. U.S. Patent 4,410,501, 1983.
64. Perego G, Bellussi G, Corno C, Taramasso M, Buonomo F, Esposito A. Titanium-silicalite: a novel derivative in the pentasil family. In: Murakami Y, Iijima A, Ward JW, eds. *New Developments in Zeolite Science and Technology, Proceedings of the 7th International Zeolite Conference*. Vol. 28. Tokyo, Japan: Elsevier Science Publ B V, 1986:129–136.
65. Dartt CB, Davis ME. Characterization and catalytic activity of titanium containing SSZ-33 and aluminum-free zeolite Beta. *Appl Catal A*. 1996;143(1):53–73.
66. Camblor MA, Corma A, Martinez A, Perez-Pariente J. Synthesis of a titaniumsilicoaluminate isomorphous to zeolite-Beta and its application as a catalyst for the selective oxidation of large organic molecules. *J Chem Soc-Chem Commun*. 1992(8):589–590.
67. Corma A, Navarro MT, Perez-Pariente J. Synthesis of an ultralarge pore titanium silicate isomorphous to MCM-41 and its application as a catalyst for selective oxidation of hydrocarbons. *J Chem Soc-Chem Commun*. 1994(2):147–148.
68. Clerici MG, Bellussi G, Romano U. Synthesis of propylene-oxide from propylene and hydrogen-peroxide catalyzed by titanium silicalite. *J Catal*. 1991;129(1):159–167.
69. Clerici MG, Ingallina P. Epoxidation of lower olefins with hydrogen-peroxide and titanium silicalite. *J Catal*. 1993;140(1):71–83.
70. Langhendries G, De Vos DE, Baron GV, Jacobs PA. Quantitative sorption experiments on Ti-zeolites and relation with alpha-olefin oxidation by H_2O_2. *J Catal*. 1999;187(2):453–463.
71. Clerici MG. The role of the solvent in TS-1 chemistry: active or passive? An early study revisited. *Top Catal*. 2001;15(2–4):257–263.
72. De Vos DE, Denayer J, van Laar F, Baron GV, Jacobs PA. Tracer chromatographic adsorption studies in relation to liquid-phase catalysis. *Top Catal*. 2003;23(1–4):191–198.
73. Ramachandran CE, Du HW, Kim YJ, Kung MC, Snurr RQ, Broadbelt LJ. Solvent effects in the epoxidation reaction of 1-hexene with titanium silicalite-1 catalyst. *J Catal*. 2008;253(1):148–158.
74. Bhosale SH, Rao MB, Deshpande VV. Molecular and industrial aspects of glucose isomerase. *Microbiol Rev*. 1996;60(2):280–300.
75. Topper YJ. On the mechanism of action of phosphoglucose isomerase and phosphomannose isomerase. *J Biol Chem*. 1957;225(1):419–425.
76. Dyson JED, Noltmann EA. Effect of pH and temperature on kinetic parameters of phosphoglucose isomerase – participation of histidine and lysine in a proposed dual function mechanism. *J Biol Chem*. 1968;243(7):1401–1414.
77. Collyer CA, Blow DM. Observations of reaction intermediates and the mechanism of aldose-ketose interconversion by D-xylose isomerase. *Proc Natl Acad Sci. USA*. 1990;87(4):1362–1366.
78. Kovalevsky AY, Hanson L, Fisher SZ, Mustyakimov M, Mason SA, Forsyth VT, Blakeley MP, Keen DA, Wagner T, Carrell HL, Katz AK, Glusker JP, Langan P. Metal ion roles and the movement of hydrogen during reaction catalyzed by D-xylose isomerase: a joint X-ray and neutron diffraction study. *Structure*. 2010;18(6):688–699.
79. Li SG, Tuan VA, Falconer JL, Noble RD. Separation of 1,3-propanediol from glycerol and glucose using a ZSM-5 zeolite membrane. *J Membr Sci*. 2001;191(1–2):53–59.
80. Camblor MA, Corma A, Perez-Pariente J. Synthesis of titanoaluminosilicates isomorphous to zeolite Beta, active as oxidation catalysts. *Zeolites*. 1993;13(2):82–87.
81. Corma A, Domine ME, Nemeth L, Valencia S. Al-free Sn-Beta zeolite as a catalyst for the selective reduction of carbonyl compounds (Meerwein-Ponndorf-Verley reaction). *J Am Chem Soc*. 2002; 124(13):3194–3195.
82. Corma A, Nemeth LT, Renz M, Valencia S. Sn-zeolite Beta as a heterogeneous chemoselective catalyst for Baeyer-Villiger oxidations. *Nature*. 2001;412(6845):423–425.
83. Bermejo-Deval R, Assary RS, Nikolla E, Moliner M, Román-Leshkov Y, Hwang S-J, Palsdottir A, Silverman D, Lobo RF, Curtiss LA, Davis ME. Metalloenzyme-like catalyzed isomerizations of sugars by Lewis acid zeolites. *Proc Natl Acad Sci USA*. 2012;109(25):9727–9732.
84. Román-Leshkov Y, Moliner M, Labinger JA, Davis ME. Mechanism of glucose isomerization using a solid Lewis acid catalyst in water. *Angew Chem Int Ed*. 2010;49(47):8954–8957.
85. Cheng L, Curtiss LA, Assary RS, Greeley J, Kerber T, Sauer J. Adsorption and diffusion of fructose in zeolite HZSM-5: Selection of models and methods for computational studies. *J Phys Chem C*. 2011;115(44):21785–21790.
86. Galema SA, Hoiland H. Stereochemical aspects of hydration of carbohydrates in aqueous solutions. 3. Density and ultrasound measurements. *J Phys Chem*. 1991;95(13):5321–5326.
87. Bock K, Meldal M, Meyer B, Wiebe L. Isomerization of D-glucose with glucose-isomerase – a mechanistic study. *Acta Chem Scand Ser B*. 1983;37(2):101–108.

Manuscript received Oct. 30, 2012, and revision received Dec. 10, 2012.